BHR Group

EXPERTS IN FLUID ENGINEERING

Simplified mechanistic model for the separation of dispersed oil-water horizontal pipe flows

Nikola Evripidou, Victor Voulgaropoulos*, Panagiota Angeli+
ThAMeS Multiphase Research Group, Department of Chemical Engineering,
University College London, London WC1E 7JE, UK
*currently at Department of Chemical Engineering, Imperial College London,
London SW7 2AZ, UK
+corresponding author, p.angeli@ucl.ac.uk

A mechanistic model that predicts the separation of oil-water dispersed horizontal pipe flows was investigated. Different droplet diameter averages were implemented in the model and the accuracy of the resulting predictions was assessed by comparing each case against experimental data. The experimental data used was obtained in a pilot scale two-phase flow facility using tap water and oil (828 kg m^{-3}, 5.5 mPa s) as test fluids. The results show that the separation length is highly sensitive to the drop diameter, but further investigation is required to determine which drop diameter average produces more accurate predictions of the flow profile.

1   INTRODUCTION

The study of the separation dynamics of oil/water dispersions is of significant importance to the petroleum industry. Such dispersions are often formed on offshore platforms during pressure reduction and may be stabilised by surfactants found naturally in crude oil. Nevertheless, the density difference between the phases is often enough to cause separation which eventually leads to stratification. This is especially the case during transportation of the extracted crude oil over long distances, for example from the offshore platform to the refinery, and in pipe separators where low velocities exist.

In the last century, oil/water mixtures have been studied extensively. Model oils have been used in laboratories to allow observation and identification of different flow patterns (1), (2), (3), (4), (5), (6). The separation dynamics of liquid-liquid mixtures have also been studied in static settlers and some models have been developed (7), (8), (9), (10). The study of the separation of liquid-liquid pipe flows, however, is a relatively new area of research (6), (11), (12), (13).

This paper presents a model that predicts the average droplet size, the formation and evolution of the continuous layers in the axial direction, as well as the pipe length required for stratification. The model was developed by Henschke et al. (10) for batch dispersions and has been modified to accommodate pipe flow. Using the model, a parametric study was performed investigating the effect of the dispersed phase droplet size on the separation dynamics.

2   NOMENCLATURE

Latin

A	Cross-sectional area (m^2)
Ar	Archimedes number (-)
C_f	Coefficient for hindered flotation (-)
C_w	Modified friction coefficient (-)
C_1, C_2	Coefficients obtained on the basis of continuity (-)
d	Drop diameter (m)
g	Gravitational acceleration (m s^{-2})
h	Layer thickness (m)
H	Hamaker coefficient (N m)
K_{HR}	Hadamard-Rybczynski factor (-)
La	Laplace number (-)
r_a	Channel contour radius (m)
$r_{F,C}$	Drop-drop contact radius (m)
$r_{F,I}$	Drop-interface contact radius (m)
r_V^*	Parameter describing the asymmetry of the film between adjacent drops (-)
Re	Reynolds number (-)
u	Velocity (m s^{-1})
x	Distance in the axial direction of the flow downstream of the inlet (m)
y	Distance in the vertical direction of the flow from the bottom of the pipe (m)

Greek

ξ	Flotation parameter (-)
λ	Flotation parameter (-)
μ	Viscosity (Pa s)
ρ	Density (kg m^{-3})
$\Delta\rho$	Density difference between the two phases (kg m^{-3})
σ	Interfacial tension (N m^{-1})
τ_C	Drop-drop coalescence time (s)
τ_I	Drop-interface coalescence time (s)
φ	Oil phase fraction (-)

Superscripts & Subscripts

∞	Infinity

+	Non-dimensionalised variable
'	Denotes the length at which flotation completes
0	Initial
32	Sauter mean
50	50th percentile
C	Continuous phase
D	Initially dispersed phase
I	Interface
M	Mixture
o	Oil phase
p	Drop
P	Dense-packed layer
sep	Separation
w	Water

3   MODEL DESCRIPTION

As a dispersion flows along a pipe, four characteristic layers can be observed: a pure layer of the continuous phase, a sedimentation zone, a dense-packed zone, and a continuous layer of the initially dispersed phase (see Figure 1 for an initial dispersion of oil drops in water). The width of each layer depends on the droplet sedimentation and interfacial coalescence rates, both of which are affected by drop coalescence.

A simplified mechanistic one-dimensional model was implemented for the prediction of the formation and evolution of the characteristic layers in the pipe, using as an example an oil-in-water dispersion. The model applies to low velocity liquid-liquid flows, where the momentum of the continuous phase is low, hence the separation process is primarily gravity-controlled. It also assumes a constant mixture velocity, u_m, for both phases along the spanwise direction — thus neglecting velocity profiles and exchange of momentum between the layers, both of which affect droplet coalescence as shown recently by Voulgaropoulos and Angeli (14). The mixture is assumed to be monodisperse with negligible surfactants present and asymmetrical film drainage is considered to happen during coalescence, as argued by Henschke et al. (10). Velocity gradients and turbulence effects due to pipe flow, and droplet break-up are not considered.

Among the available batch-separation models, the asymmetric dimple model developed by Henschke et al. (10) is thought to be the most suitable for pipe flows, as it requires calibration of a single parameter which is related to the dimensionless asymmetry of the film drainage r_V^*. According to Henschke et al. (10), for a given oil-water mixture, r_V^* is independent of: 1) initial droplet-size, 2) water-cut, and 3) batch height, thus making the scale-up from simple laboratory tests to field-scale conditions feasible.

The model combines the main mechanisms that are thought to occur during pipe flow. These include:
- Flotation
- Drop-interface coalescence

- Binary drop coalescence

The equations describing the mechanisms are solved along the length of the pipe updating the height of each characteristic layer and the droplet size for each step, eventually producing a pipe profile of the characteristic layers.

The input parameters required for the model to be consistent are:
  i. Fluid properties (densities, viscosities, surface tension)
  ii. Pipe geometry
  iii. Initial droplet size
  iv. Initial thickness of the pure water and pure oil layers.

3.1 Flotation analysis

The primary separation mechanisms acting on an oil-water mixture are density-driven sedimentation or flotation. Pilhofer and Mewes (15) developed an empirical model that computes the vertical (sedimentation/flotation) velocity of a swarm of droplets in settling experiments. This vertical velocity which was developed for a mono-dispersed system taking as the average droplet diameter the Sauter mean diameter at the pipe inlet, d_{32}^0, is described by the following expression:

$$u_{\mathrm{f}} = C_{\mathrm{f}} \frac{3\lambda\varphi\mu_{\mathrm{C}}}{C_{\mathrm{w}}\xi(1-\varphi)\rho_{\mathrm{C}}d_{\mathrm{P}}} \left[\left(1 + Ar\frac{C_{\mathrm{w}}\xi(1-\varphi)^3}{54\lambda^2\varphi^2} \right)^{0.5} - 1 \right], \tag{1}$$

where the dimensionless parameters are defined as follows:
Archimedes number, Ar:

$$Ar = \frac{\rho_{\mathrm{C}}\Delta\rho g d_{\mathrm{P}}^3}{\mu_C^2}, \tag{2}$$

flotation velocity parameter λ:

$$\lambda = \frac{1-\varphi}{2\varphi K_{\mathrm{HR}}} \exp\left(\frac{2.5\varphi}{1-0.61\varphi} \right), \tag{3}$$

flotation velocity parameter ξ:

$$\xi = 5K_{\mathrm{HR}}^{-\frac{3}{2}} \left(\frac{\varphi}{1-\varphi} \right)^{0.45}, \tag{4}$$

Hadamard-Rybczynski factor, K_{HR}:

$$K_{\mathrm{HR}} = \frac{3(\mu_{\mathrm{C}} + \mu_{\mathrm{D}})}{2\mu_{\mathrm{C}} + 3\mu_{\mathrm{D}}}, \tag{5}$$

friction coefficient, C_{w}:

$$C_{\mathrm{w}} = \frac{Ar}{6Re_\infty^2} - \frac{3}{K_{\mathrm{HR}}Re_\infty}, \tag{6}$$

Reynolds number of a single droplet moving vertically in an infinite medium, Re_∞:

$$Re_\infty = \frac{\rho_C u_f^\infty d_P}{\mu_C} = 9.72\left[(1 + 0.01Ar)^{\frac{4}{7}} - 1\right]. \tag{7}$$

The height of the flotation curve of a given mixture can then be predicted by:

$$h_c = \frac{u_f x}{u_M}. \tag{8}$$

3.2 Coalescence Analysis

As the oil droplets float towards the top of the pipe coalescence occurs, forming a continuous oil layer with thickness, h_D. The rate of change of h_D with time is determined by the rate of coalescence of droplets with the flat interface. Assuming a monodispersed mixture at the interface, where all droplets have the same diameter d_{32}^I, and using the geometry presented in Figure 1, Pereyra (11) showed that the evolution of the oil layer can be defined as follows:

$$u_M \frac{dh_D}{dx} = \frac{2\varphi_I d_{32}^I}{3\tau_I}, \tag{9}$$

where φ_I is the dispersed-phase fraction at the interface and is approximately equal to 1 while τ_I is the coalescence time between a drop and the interface.

3.2.1 Evolution of droplet sizes

Drop-drop coalescence is considered only in the dense-packed region. Assuming that during each step and at the same vertical position, all droplets are of equal size and equal to the Sauter mean diameter, d_{32}, Hartland and Jeelani (7) proposed the following expression for predicting the evolution of the droplet size as a function of the coalescence time between two drops, τ_C:

$$u_M \frac{d(d_{32})}{dx} = \frac{d_{32}}{6\tau_C}. \tag{10}$$
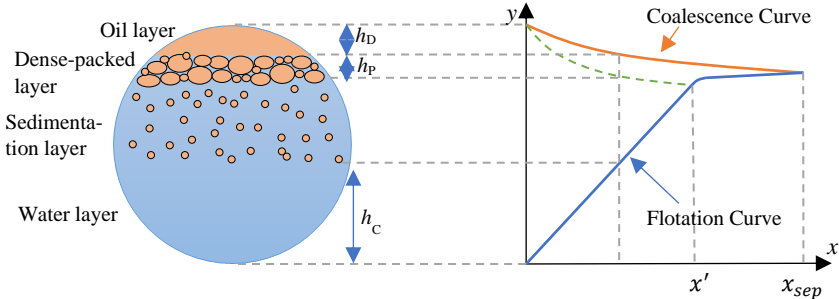
3.2.2 Evolution of dense-packed zone height

Figure 1: Diagram of the cross-sectional area of the pipe for an oil-in-water dispersion and diagram of the evolution of the characteristic layers.

The change of the height of the dense-packed zone, h_P, can be determined by mass balance at the pipe cross-sectional area. For a given oil-in-water dispersion of φ_0 initial dispersed-phase fraction, there exists an axial distance x' where the sedimentation of droplets is completed, and the dense-packed zone thickness begins to decrease (see Figure 1). Upstream of this location ($0 < x < x'$), the cross-sectional area of the dense-packed zone is given by:

$$A_P = \frac{(A_C \varphi_0 - (1 - \varphi_0)A_D)}{\varphi_{P,0} - \varphi_0}. \tag{11}$$

Once the sedimentation process is completed ($x > x'$), equation (11) simplifies to:

$$A_P = \frac{(A_{pipe}\varphi_0 - A_D)}{\varphi_P'}, \tag{12}$$

where the average holdup in the dense-packed zone, φ_P', is a function of axial position and can be estimated by the following equation:

$$\varphi_P' = \varphi_I - \exp\left(-C_1 \frac{x}{u_M} - C_2\right). \tag{13}$$

C_1 and C_2 are coefficients determined based on continuity. At $x = x'$, $\varphi_P' = \varphi_{P,0}$ and the two coefficients are given by:

$$C_1 = \frac{{\varphi_{P,0}'}^2 \psi}{(A_{pipe}\varphi_0 - A_D)(\varphi_I - \varphi_{P,0})} \tag{14}$$

and

$$C_2 = -C_1 \frac{x'}{u_M} - \ln(\varphi_I - \varphi_{P,0}), \tag{15}$$

where

$$\psi = \left[\frac{\partial A_P}{\partial h_P}\left(u_f + u_M \frac{dh_D}{dx}\right) - \frac{u_M}{\varphi_{P0}'}\frac{\partial A_D}{\partial h_D}\frac{\partial h_D}{\partial x} - u_M \frac{\partial A_P}{\partial h_D}\frac{\partial h_D}{\partial x}\right]_{x=x'}. \tag{16}$$

3.2.3   Coalescence Time
Modelling the coalescence process requires knowledge of the initial droplet-size distribution in the dense-packed zone, which depends on both the size of the droplets and their deformation. The droplet deformation increases with the thickness of the dense-packed zone. Henschke (16) solved the equations describing droplet deformation numerically and derived the following empirical formulae:

droplet/droplet contact area radius, $r_{F,C}$:

$$r_{\text{F,C}} = 0.3025 \, d_{32} \sqrt{1 - \frac{4.7}{La + 4.7}}, \tag{17}$$

channel contour radius, r_{a}:

$$r_{\text{a}} = 0.5 \, d_{32} \left(1 - \sqrt{1 - \frac{4.7}{La + 4.7}} \right), \tag{18}$$

where La is a modified Laplace number that accounts for the close packing of drops and is given as follows:

$$La = \left(\frac{|\rho_{\text{D}} - \rho_{\text{C}}| g}{\sigma} \right)^{0.6} h_{\text{P}}^{0.2} \, d_{32}. \tag{19}$$

For drop/interface coalescence the following approximation can be used for the contact area radius, $r_{\text{F,I}}$:

$$r_{\text{F,I}} = \sqrt{3} \, r_{\text{F,C}}. \tag{20}$$

On the basis of an asymmetric film-drainage analysis, Henschke et al. (10) suggested that the binary droplet coalescence time of droplets with diameter d_{32} could be computed as follows:

$$\tau_{\text{C}} = \frac{(6\pi)^{\frac{7}{6}} \mu_{\text{C}} \, r_{\text{a}}^{\frac{7}{3}}}{4\sigma^{\frac{5}{6}} H^{\frac{1}{6}} r_{\text{F,C}} r_{\text{V}}^*} \tag{21}$$

and the droplet-interface coalescence time of a single droplet of diameter d_{32} by modifying equation (21):

$$\tau_{\text{I}} = \frac{(6\pi)^{\frac{7}{6}} \mu_{\text{C}} \, r_{\text{a}}^{\frac{7}{3}}}{4\sigma^{\frac{5}{6}} H^{\frac{1}{6}} r_{\text{F,I}} r_{\text{V}}^*}. \tag{22}$$

The equations above contain two unknown parameters: the asymmetry parameter, r_{V}^*, and the Hamaker coefficient, H. The asymmetry parameter can be obtained from experimental flotation curves and is characteristic for the system used. The Hamaker coefficient is set to 10^{-20} N m, as proposed by Henschke et al. (10) for any system.

3.2.4   Length of Segregation
The length required to reach complete separation of the two phases can be determined from the intersection point between the coalescence curve and the flotation curve, as given by equation (12).

4 RESULTS AND DISCUSSION

4.1 Experimental methods

Experimental data were obtained in a liquid-liquid flow facility discussed in detail in Voulgaropoulos (6) and Voulgaropoulos et al. (17). Tap water and oil (828 kg m^{-3}, 5.5 mPa s) were employed as test fluids. The test section consisted of 37 mm internal diameter transparent acrylic pipes with overall length of about 8 m. A multi-nozzle mixer was used to generate the dispersions at the inlet of the test section. The flow patterns were identified with high-speed imaging at three axial locations along the pipe. Measurements of the local volume fractions and drop size distributions of oil-in-water dispersions were obtained using a dual-conductance probe. Measurements were performed every 2 mm, spanning the whole pipe spanwise diameter.
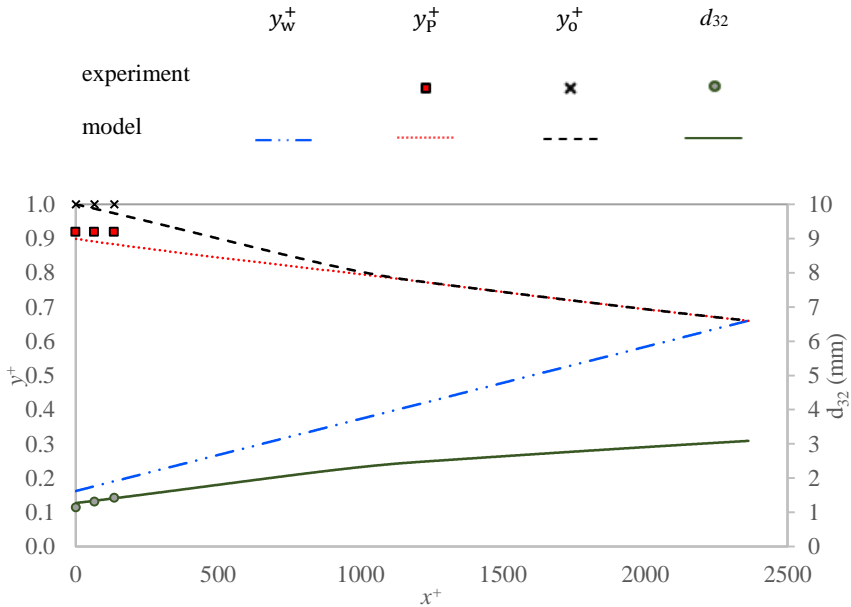
4.2 Model performance

Figure 2: Prediction of the evolution of the characteristic layers and the Sauter mean diameter at $u_m = 1$ ms^{-1} and $\varphi_0 = 0.30$ and comparison with experimental measurements.

The model performance was assessed by recreating Figure 4.21(b) in Voulgaropoulos (6). Although the pilot-scale facility allowed only three measurements to be taken along the axial length of the pipe, figure 2 shows that the model predicts changes in the heights of the dense-packed layer interfaces with small deviations from experimental results. The evolution of the drop sizes is also captured to an adequate extent using $r_V^* = 0.007$, a value that was obtained experimentally by Pereyra et al. (12) for a similar system.

4.3 Quantitative assessment of different average drop diameters

As previously mentioned, the asymmetric dimple model makes use of the Sauter mean diameter, d_{32}. According to Voulgaropoulos (6), d_{32} is biased towards larger drop sizes in

log-normal distributions, hence even few very large droplets can result to a significant increase in d_{32}. In this paper, the accuracy of the results produced using d_{32} is assessed. Flow profiles were obtained using d_{32}, the arithmetic mean diameter, d_{mean}, the median diameter, d_{50}, and the mode diameter, d_{mode}. It is worth mentioning that d_{32} and d_{mean} were taken directly from the experiments of Voulgaropoulos (6), while d_{mode} and d_{50} were extracted from the probability density functions to drop size distributions in Voulgaropoulos (6).
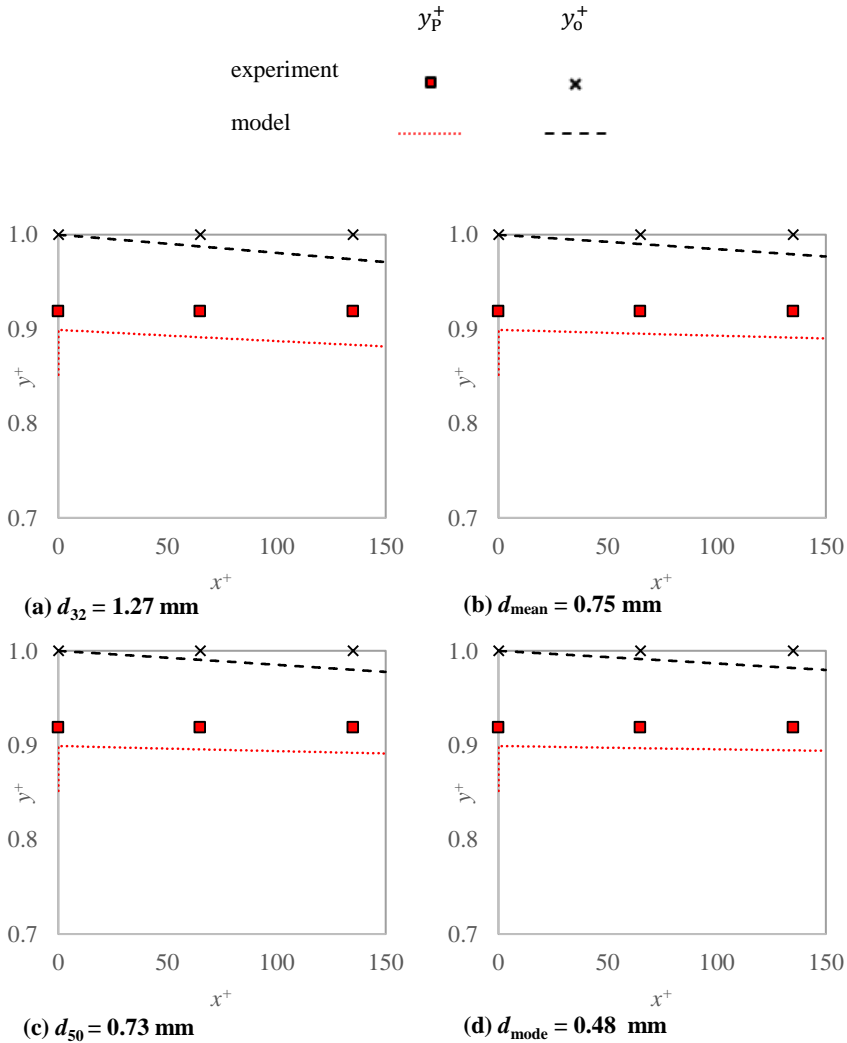

Figure 3: Prediction of the coalescence curve and interface between the sedimentation and dense-packed zones using different initial drop size diameter averages (from left to right, top to bottom: $d_{32} = 1.27$ mm, $d_{mean} = 0.75$ mm, $d_{50} = 0.73$ mm, $d_{mode} = 0.48$ mm) for $0 < x^+ < 150$ and comparison with experimental measurements.

Figure 3 shows that although the largest errors were obtained using d_{32}, height differences between each case are negligible. In all cases however, the model appeared to overestimate coalescence, as for every drop diameter average, the oil layer thickness was predicted to increase at a higher rate than observed. The rate of change of height of the interface between the sedimentation and dense-packed zones was also overestimated.

Table 1: Percentage error of model predictions at $x^+ = 65$ and 135 using different drop diameter averages.

Drop Average	Percentage error in coalescence curve height (%)		Percentage error in sedimentation/ dense-packed zone interface height (%)	
	$x^+ = 65$	$x^+ = 135$	$x^+ = 65$	$x^+ = 135$
d_{32}	1.25	2.62	3.00	3.88
d_{mean}	0.99	2.08	2.59	3.04
d_{50}	0.96	2.01	2.54	2.93
d_{mode}	0.87	1.83	2.40	2.65

Table 1 was included to enable a quantitative comparison between the modelling and experimental results. It can be seen that the d_{32} produces the largest error out of all the drop diameter averages, while d_{mode} has the best performance. Nevertheless, percentage errors in the heights of the dense-packed zone interfaces are very small (<4%) and within experimental uncertainty, regardless of the drop diameter average used.

Data in Table 1 suggest that the small differences in the parameters in the beginning of the pipe can have a large impact on the separation as the mixture flows along the axial distance. Consequently, even small improvements in the accuracy of the model near the inlet may have significant impact in the overall flow profile and the total length required for complete separation, which is expected to be an order of magnitude larger than the length studied in the pilot scale experiments.

Table 2: Predicted total length required for separation for different drop diameters.

Drop Average	Separation length, x^+_{sep}
d_{32}	2360
d_{mean}	4410
d_{50}	4980
d_{mode}	7410

To determine the sensitivity of the model to the drop size, the effect of the drop diameter on the total length required for complete separation, x^+_{sep}, was investigated. The results, which are summarised in Table 2, show that the drop diameter has a significant impact on the separation length. Comparing the results for d_{50} and d_{32}, it can be seen that the

separation length more than doubles when the drop diameter increases by a factor of 1.7. Similarly, an increase in the drop diameter by a factor of 2.6 results in a separation length that is more than thrice the initial value, as can be seen by the comparison between d_{mode} and d_{32}. It is therefore apparent that the length required for complete segregation is highly sensitive to the drop diameter, thus the drop average used in the model must be carefully selected.

5   CONCLUSIONS

The paper presents one of the possible models that can be used to predict the separation behaviour of dispersed oil-water pipe flows. Although, there could be other legitimate approaches (13), the phenomenological model presented here captures the main mechanisms of the separation of dispersed oil-water pipe flows adequately within 4% of the experimental data. Sensitivity analysis of the effect of drop size on the total separation length showed that the separation length is highly sensitive to the drop diameter. Assessment of the drop diameter averages did not result in any statistically valid conclusions; thus further investigation is required to determine which average produces more accurate predictions of the evolution of the characteristic layers and the overall length required for the separation of the dispersion when a single droplet size approach is used for modelling simplifying purposes.

Acknowledgements

6   REFERENCES

(1)   Angeli, P., Hewitt, G.F., 2000. Flow structure in horizontal oil-water flow. Int J Multiphase Flow 26, 1117-1140.

(2)   Elseth, G., 2001. An experimental study of oil/water flow in horizontal pipes. Norwegian University of Science and Technology, Trondheim, Norway.

(3)   Lovick, J., Angeli, P., 2004. Droplet size and velocity profiles in liquid-liquid horizontal flows. Chem Eng Sci 59, 3105-3115.

(4)   Simmons, M.J.H., Azzopardi, B.J., 2001. Drop size distributions in dispersed liquid-liquid pipe flow. Int J Multiphase Flow 27, 843-859.

(5)   Trallero, J. L., Sarica, C., Brill. J. P., 1997. A study of oil-water flow patterns in horizontal pipes. SPE Production & Facilities 12 (03): 165–72.

(6)   Voulgaropoulos, V., 2018. Dynamics of spatially evolving dispersed flows. PhD dissertation, University College London, London, UK.

(7)   Hartland, S., Jeelani, S. A. K., 1988. Prediction of sedimentation and coalescence profiles in a decaying batch dispersion. Chemical Engineering Science 43, 2421-2429.

(8)   Jeelani, S. A. K., Hartland, S., 1998. Effect of dispersion properties on the separation of batch liquid-liquid dispersions. Ind. Eng. Chem. Res. 37, 547-554.

(9)   Jeelani, S. A. K., Panoussopoulos, K., Hartland, S., 1999. Effect of turbulence on the separation of liquid-liquid batch settlers of different geometries. Ind. Eng. Chem. Res. 38, 493-501.

(10) Henschke, M., Schlieper, L.H., Pfennig, A., 2002. Determination of a coalescence parameter from batch-settling experiments. Chem Eng J 85, 369-378.

(11) Pereyra, E., 2011 Modelling of compact multiphase separation system (CMSS©). PhD dissertation, The University of Tulsa, Tulsa, Oklahoma, USA.

(12) Pereyra, E., Mohan, R.S., Shoham, O., 2013. A simplified mechanistic model for an oil/water horizontal pipe separator. Oil and Gas Facilities, 2 (03): 40-46.

(13) Othman, H. A. Dabirian, R., Gavrielatos, R., Mohan, R., Shoham, O., 2018. Validation and improvement of the horizontal pipe separator (HPS©) in SPE Western Regional Meeting. Society of Petroleum Engineers. Garden Grove, 22-26 April.

(14) Voulgaropoulos, V., Angeli, P., 2017. Optical measurements in evolving dispersed pipe flows. Experiments in Fluids, 58, 170.

(15) Pilhofer, T., Mewes, D., 1979. Siebboden-Extraktionskolonnen: Vorausberechnung unpulsierter Kolonnen. Verlag Chemie.

(16) Henschke, M., 1995. Dimensionierung liegender Flüssig–flüssig Abscheider nhand diskontinuierlicher Absetzversuche, Fortschritt-Berichte VDI, Reihe 3, Nr. 379, VDI-Verlag, Düsseldorf.

(17) Voulgaropoulos, V., Zhai, L.-S., Ioannou, K., Angeli, P., 2016. Evolution of unstable liquid-liquid dispersions in horizontal pipes. 10th North American Conference on Multiphase Technology. BHR Group. Banff, 8-10 June.